Journal of Applied Electrochemistry **29**: 1323–1327, 1999.

Characteristics of $La_{0.65}Nd_{0.2}Pr_{0.15}Ni_{3.55}Co_{0.75}Mn_{0.4}Al_{0.3}$ electrode for nickel metal hydride batteries

H.M. JIN[1]*, G.X. LI[2], R.K. WANG[2], C.H. ZHOU[2] and P. WU[3]
[1]*Department of Materials Science, National University of Singapore, Singapore 119260;*
[2]*General Research Institute for Non-ferrous Metals, Beijing 100088;*
[3]*Institute of High Performance Computing, 89B Science Park Drive 01-05/08, Singapore 118261*
*(*author for correspondence at Institute of High Performance Computing, 89B Science Park Drive, 01-05/08, Singapore 118261, e-mail: jinhm@ihpc.nus.edu.sg)*

Received 19 October 1998; accepted in revised form 27 May 1999

Key words: activation, charge–discharge capabilities, cycle life, negative electrode

Abstract

The discharge capacity, high rate capability and cycle life degradation of the $La_{0.65}Nd_{0.2}Pr_{0.15}Ni_{3.55}Co_{0.75}Mn_{0.4}Al_{0.3}$ electrode have been investigated. The electrochemical properties of the electrode are significantly improved by partial replacement of La by Nd and Pr. The cycle life degradation of the electrode are examined by using analytical electron microscopy (AEM). Results show that the alloy particles of the negative electrode are gradually oxidized during the charge–discharge process. Microanalysis of the oxidized layer reveals that the oxidation layer is mainly composed of $La(OH)_3$ and oxides of Nd, Mn and Al. Further observation of the particle morphology after 400 cycles shows that the oxidation layer becomes loose during cycling. The loose oxides cannot protect particles from further electrolytic attack. This may lead to the decrease of the discharge capacity.

1. Introduction

Multicomponent nickel/metal hydride batteries offer solutions to many problems associated with the production, application and disposal of nickel–cadmium batteries. Since the $LaNi_5$ electrode corrodes and pulverizes rapidly during charge discharge cycling, much research [1–5] has been focused on the partial replacement of Ni by third elements such as Co, Al, Mn, Si, Ge and Sn, but relatively little work has been reported about the effects of La substitution. It is proposed that optimization of La substitution (similar to Ni substitution) may be an effective approach to further improve the capabilities of the negative electrode.

In our research, a range of $La_{1-x}Nd_xNi_{3.55}Co_{0.75}Mn_{0.4}Al_{0.3}$ and $La_{1-x}Pr_xNi_{3.55}Co_{0.75}Mn_{0.4}Al_{0.3}$ alloys were prepared by partially replacing La with Pr or Nd. The discharge capacity, high rate capability and cycle life stability of the electrodes have been investigated and results are listed in Table 1. It can be seen that the discharge capacity increased with increasing x (Nd and Pr contents), and reached a maximum value when the content of Nd or Pr is 0.2 at %. When the content of Nd or Pr is larger than 0.2 at %, the discharge capacity decreased. In addition, the high rate capability of $La_{1-x}Nd_xNi_{3.55}Co_{0.75}Mn_{0.4}Al_{0.3}$ and $La_{1-x}Pr_xNi_{3.55}Co_{0.75}Mn_{0.4}Al_{0.3}$ electrodes was found to decrease with increasing Nd or Pr contents. For $La_{1-x}Nd_xNi_{3.55}Co_{0.75}Mn_{0.4}Al_{0.3}$ electrodes the cycle life was improved with increasing Nd content. For $La_{1-x}Pr_xNi_{3.55}Co_{0.75}Mn_{0.4}Al_{0.3}$ electrodes, the effect of Pr on cycle life was insignificant.

In this paper a $La_{0.65}Nd_{0.2}Pr_{0.15}Ni_{3.55}Co_{0.75}Mn_{0.4}Al_{0.3}$ alloy was used as raw materials. The hydrogen desorption ability of the alloy, the charge–discharge capabilities and cycle life degradation mechanism of the electrode were investigated.

2. Experimental details

The $La_{0.65}Nd_{0.2}Pr_{0.15}Ni_{3.55}Co_{0.75}Mn_{0.4}Al_{0.3}$ alloy was prepared by arc-melting a mixture of the high purity metals under argon. The alloy was re-melted several times to ensure homogeneity. Pressure composition isotherms (PCT curve) were measured using a home-built [6] testing instrument. The molar volume of hydrogen in the hydride phase was determined via gas–solid reaction at 30 °C and under a H_2 pressure of about 1.9 MPa.

For the discharge capacity, the alloy powder was mixed with fine Cu powder at a weight ratio of 1:4. The mixture was pressed (at a pressure of 3×10^7 N m^{-2}) into a disc 1 g (mass) × 13 mm (dia.) × 1.1 mm (thickness). Before the experiment, the sample was immersed in a 6 M KOH electrolyte for at least 12 h. $Ni(OH)_2$/NiOOH and Hg/HgO were used as the counter electrode

Table 1. Discharge capacity, high rate capability and capacity retention for $La_xNd_{1-x}Ni_{3.55}Co_{0.75}Mn_{0.4}Al_{0.3}$ and $La_xPr_{1-x}Ni_{3.55}Co_{0.75}$ $Mn_{0.4}Al_{0.3}$ electrodes

Alloy composition	Discharge capacity C_{max}/mA h g^{-1}	High rate capability, C_i/C_{max}/% Discharge current/mA g^{-1}				Capacity retention C_{350}/C_{max} (%)
		300	500	700	900	
$La_{0.9}Nd_{0.1}B_5$	265	90	88	83	79	72
$La_{0.8}Nd_{0.2}B_5$	290	87	82	75	72	75
$La_{0.7}Nd_{0.3}B_5$	286	82	73	65	60	79
$La_{0.6}Nd_{0.4}B_5$	248	81	73	65	58	80
$La_{0.4}Nd_{0.6}B_5$	221	78	72	63	54	90
$La_{0.2}Nd_{0.8}B_5$	200	78	68	58	53	96
$La_{0.85}Pr_{0.15}B_5$	286	96	92	85	80	76
$La_{0.8}Pr_{0.2}B_5$	291	88	82	76	73	77
$La_{0.7}Pr_{0.3}B_5$	276	84	73	65	58	78.5
$La_{0.3}Pr_{0.7}B_5$	273	75	64	58	49	80.5

C_i discharge capacity at the current of i (mA g^{-1}); C_{350} discharge capacity after 350 cycles;
B_5 $Ni_{3.55}Co_{0.75}Mn_{0.4}Al_{0.3}$

and reference electrode, respectively. For discharge capacity, the negative electrode was charged for 2 h at 200 mA g^{-1}, and then discharged to −0.65 V at 100 mA g^{-1} against the Hg/HgO electrode.

For the cycle life testing the electrode was prepared by mixing 200–300 mesh alloy with appropriate PVA and PTFE additives. The mixture was then pressed onto a 2 cm × 2 cm nickel mesh screen. It was then sandwiched between two positive $Ni(OH)_2$/NiOOH electrodes. The electrode was charged for 2.33 h at 150 mA g^{-1} and discharged at a current of 150 mA g^{-1} to −0.9 V.

The relative element concentrations at the alloy surface were determined by XPS. The oxidation process of the alloy particles during charge–discharge cycling was investigated by analytical electron microscopy (AEM).

3. Results and discussion

3.1. *Pressure composition isotherm*

The pressure composition isotherm (PCT curve) is an important parameter in the evaluation of the battery material. If the plateau pressure is too high, the alloy will be unstable after hydrogen absorption, causing problems for battery sealing. If the plateau pressure is too low, the hydrogen desorption will be difficult, and the discharge capacity will be low. A rule of thumb is that the plateau pressure should be between 0–0.1 MPa.

Figure 1 shows the desorption PCT curve of $La_{0.65}Nd_{0.2}Pr_{0.15}Ni_{3.55}Co_{0.75}Mn_{0.4}Al_{0.3}$ alloy at 30 °C. For comparison, PCT curves of the other two alloys are also included. It can be seen that the plateau pressures for the three alloys are about $0.03 \sim 0.04$ MPa. The maximum H content is about 0.9 (H/M) for the alloy with the composition $La_{0.65}Nd_{0.2}Pr_{0.15}Ni_{3.55}Co_{0.75}$-$Mn_{0.4}Al_{0.3}$. These results indicate that the $La_{0.65}Nd_{0.2}$-$Pr_{0.15}Ni_{3.55}Co_{0.75}Mn_{0.4}Al_{0.3}$ alloy may be used as battery material based on the PCT data. In addition, although the change of plateau pressure for $La_{0.65}Nd_{0.2}Pr_{0.15}$-$Ni_{3.55}Co_{0.75}Mn_{0.4}Al_{0.3}$ alloy is insignificant, the maximum hydrogen content is relatively higher.

3.2. *Alloy activation*

In the measurement of the PCT curve of $La_{0.65}Nd_{0.2}$-$Pr_{0.15}Ni_{3.55}Co_{0.75}Mn_{0.4}Al_{0.3}$ alloy it was found that the alloy is easily activated. At 30 °C and 1.9 MPa H_2 pressure, it took less than 1 min to be activated. To investigate the mechanism of activation, the surface composition of the alloy was examined using XPS. The analytical results show that on the alloy surface, elements such as La, Al, Mn and Co are in the form of oxides, but Ni remains as pure metal. The existence of pure nickel may be a possible reason for the fast activation of the alloy. Further experimental work remains to be done.

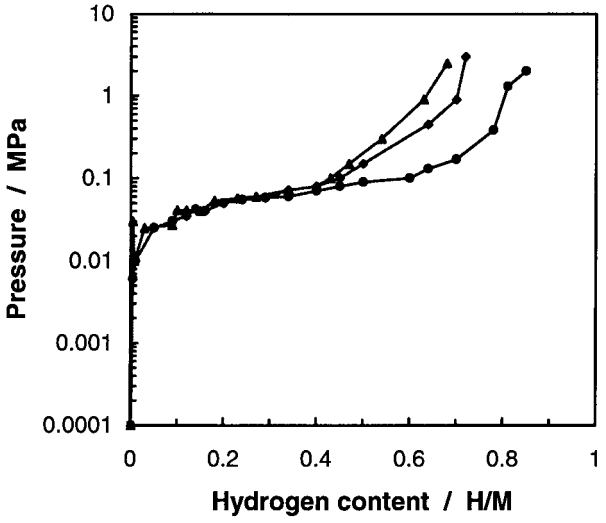

Fig. 1. Desorption pc-isotherm of alloys at 30 °C Key: (●) $La_{0.65}Nd_{0.2}Pr_{0.15}B_5$; (◆) $La_{0.8}Nd_{0.2}B_5$; (▲) $La_{0.85}Pr_{0.15}B_5$.

3.3. *High rate capability and cycle life*

Figure 2 shows discharge current dependence on discharge capacity. From this it can be seen that by increasing the discharge current, the discharge capacity decreases. However, compared to the discharge capacity of $La_{0.8}Nd_{0.2}Ni_{3.55}Co_{0.75}Mn_{0.4}Al_{0.35}$ and $La_{0.85}Pr_{0.15}Ni_{3.55}Co_{0.75}Mn_{0.4}Al_{0.35}$ (shown in Figure 2) electrodes, the high rate capability of $La_{0.85}Pr_{0.15}Ni_{3.55}Co_{0.75}Mn_{0.4}Al_{0.35}$ is improved.

Figure 3 shows the relations between discharge capacity and the number of cycles. It can be seen that the maximum discharge capacity of the $La_{0.65}Nd_{0.2}Pr_{0.15}Ni_{3.55}Co_{0.75}Mn_{0.4}Al_{0.3}$ electrode is 301 mA h g^{-1}, higher than that of $La_{0.8}Nd_{0.2}Ni_{3.55}Co_{0.75}Mn_{0.4}Al_{0.3}$ (290 mA h g^{-1}) and $La_{0.85}Pr_{0.15}Ni_{3.55}Co_{0.75}Mn_{0.4}Al_{0.35}$ (286 mA h g^{-1}) electrodes. After about 40 cycles, the capacity decreases slowly. When the cycle number reaches 350, the capacity retention (C_{350}/C_{max}) is 82% for $La_{0.65}Nd_{0.2}Pr_{0.15}Ni_{3.55}Co_{0.75}Mn_{0.4}Al_{0.3}$ electrode. Compared to the capacity retention for $La_{0.8}Nd_{0.2}Ni_{3.55}Co_{0.75}Mn_{0.4}Al_{0.3}$ and $La_{0.85}Pr_{0.15}Ni_{3.55}Co_{0.75}Mn_{0.4}Al_{0.3}$ after 350 cycles (shown in Table 1), the cycle life of the electrode containing both Nd and Pr is improved.

3.4. *AEM observation of cycle life degradation*

Figure 4 shows the particle morphology of the $La_{0.65}Nd_{0.2}Pr_{0.15}Ni_{3.55}Co_{0.75}Mn_{0.4}Al_{0.3}$ electrode after 100, 200, 300 and 400 charge–discharge cycles, respectively. It indicates that after 100 cycles, the particle surface is slightly oxidized. The thickness of the oxidation layer is about 0.12 μm. After 200 cycles, the thickness of the oxidation layer increases to about 0.19 μm (Figure 4(b)). This indicates that the thickness of the oxidation layer gradually increases with increasing cycle number, and the average rate of increase is about 0.07 μm/100 cycles. Figure 4c shows the particle

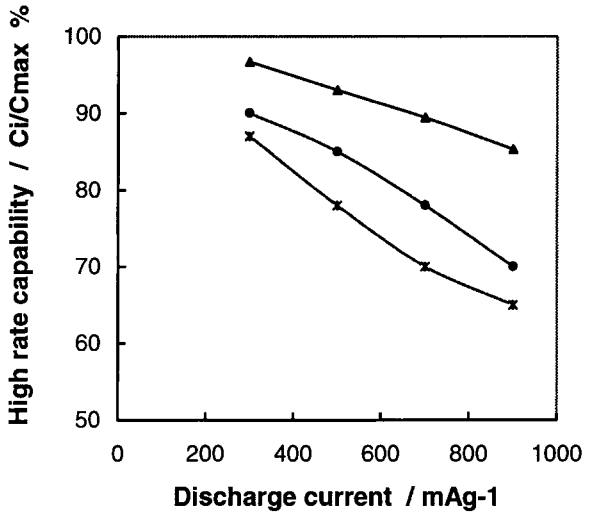

Fig. 2. Dependence of capacity on discharge current. Key: (▲) $La_{0.65}Nd_{0.2}Pr_{0.15}B_5$; (X) $La_{0.8}Nd_{0.2}B_5$; (●) $La_{0.85}Pr_{0.15}B_5$.

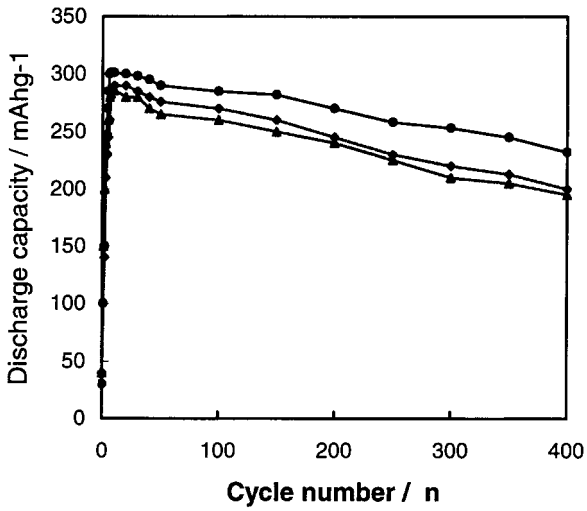

Fig. 3. Total discharge capacity against number of cycles. Key: (●) $La_{0.65}Nd_{0.2}Pr_{0.15}B_5$; (◆) $La_{0.8}Nd_{0.2}B_5$; (▲) $La_{0.85}Pr_{0.15}B_5$.

morphology after 300 cycles. The previously pulverized and oxidized particles (after 200 cycles) further pulverize into a smaller size. The diameters of these smaller particles are within the range 8–15 μm. In addition, it can also be observed that with increasing cycle number, the oxidation layer becomes porous due to the attack of the electrolyte which enters the interior of the alloy particles. Figure 4(d) displays the particles surface after 400 cycles, which indicates that the previously pulverized particles (after 300 cycles) continue to be oxidized and the thickness of oxidation layer is about 0.25 μm.

To describe the cycle life degradation process, Notten et al. [7] developed the mathematical model: $C_n = C_0 \exp(-Ak\alpha M_c n)$, where C_0 and C_n are initial discharge capacity and discharge capacity after n cycles, respectively, A is the specific area and k, α, M_c are constants. According to this model, the decline in discharge capacity depends on both the specific area and cycle times. This is theoretically in agreement with our experimental results. The specific area is proportional to the surface area of particles. The observed particle pulverization by using AEM, will increase the sum of the surface area, which will promote the oxidation rates of alloy particles and finally accelerate the degradation process of the discharge capacity.

Figure 5 shows the selected area diffraction pattern (SADP) from the interface (A area) between two particles after 100 cycles. Table 2 is the indexing result of Figure 5. It can be seen that the oxidation layer is composed of $La(OH)_3$ and oxides of La, Nd, Mn, and Al. Microanalysis of the oxidation layer and inner particles shows that there exists a large amount of oxygen. In addition, the content of Nd and Mn in the oxidation layer is about 70% less than that in the inner layer of particles. Almost all Al was dissolved into the electrolyte since the Al content is very low in the oxidation layer. These results imply that some elements like Mn, Al and rare earth elements are easily attacked by electrolyte.

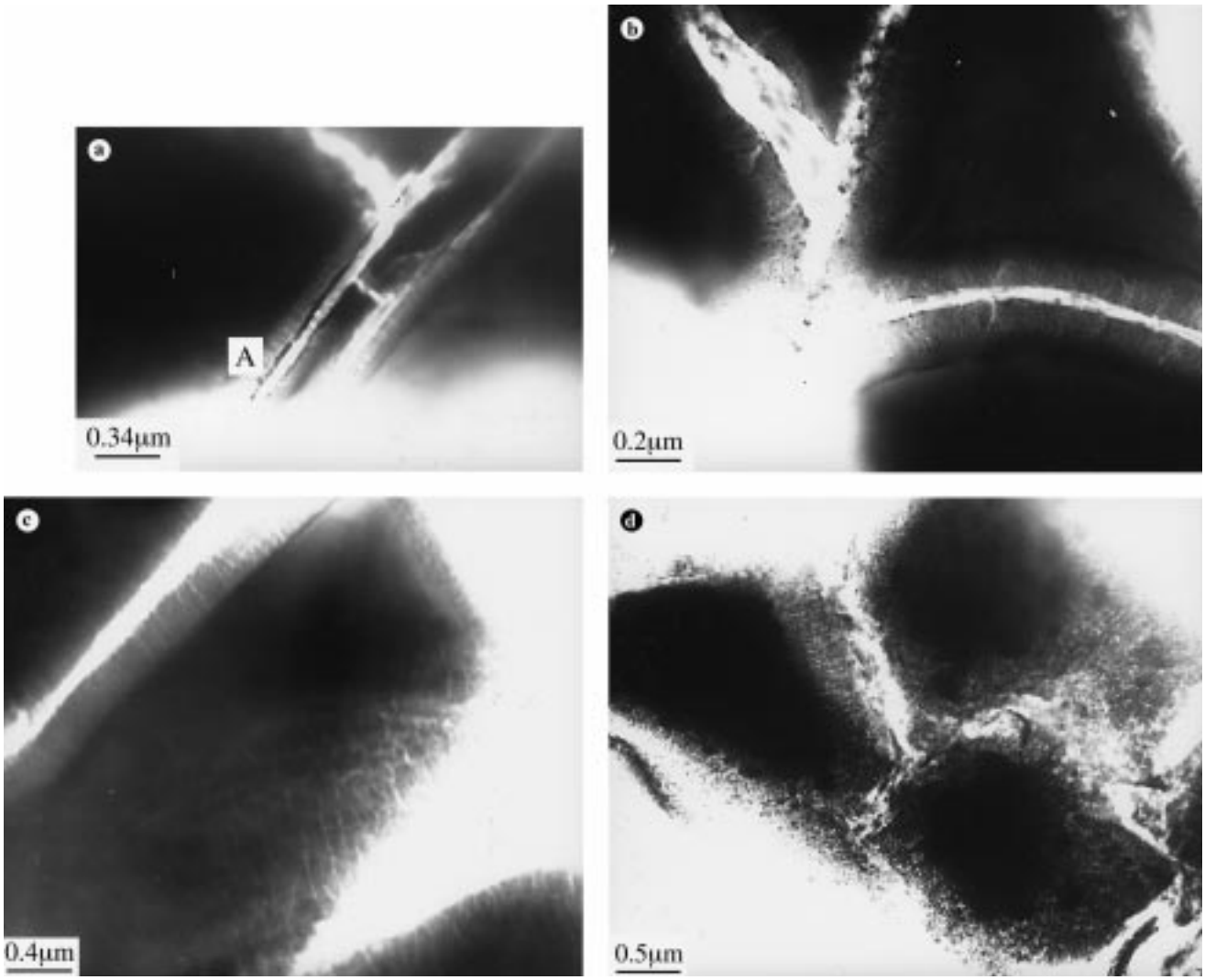

Fig. 4. Particle appearance of electrode after (a) 100, (b) 200, (c) 300 and (d) 400 cycles.

In a recent study [8], it was found that the charge–discharge capacity is strongly correlated with the diffusion properties of the constituent elements in the electrodes. This conclusion is in line with the present observations because diffusion of the chemical elements may play an important role in the formation of the observed oxides and hydroxides. Therefore, a detailed phase equilibrium study of the alloy, oxides and hydroxides system may provide useful information for the optimal design of the electrodes.

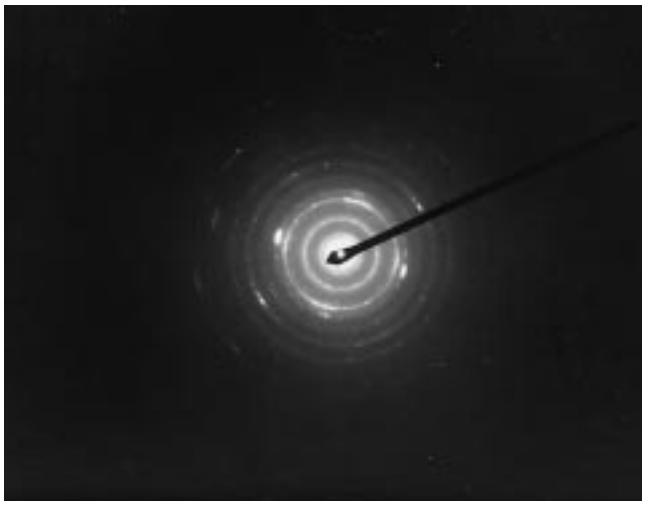

Fig. 5. Selected area diffraction pattern from interface between two particles.

Further observation of the particle surface after 400 cycles is shown in Figure 6, which shows that the oxide and hydroxide layers of the particles become weak and loose after 400 cycles. Some small cracks travel from the

Table 2. Results of selected area diffraction pattern from Figure 5

Measured value of *d* (nm)	Diffraction crystal planes of compounds				
	La_2O_3	Nd_2O_3	$La(OH)_3$	Mn_3O_8	Al_2O_3
0.320–0.350	100	210	111		102
0.189–0.212	110	440	002/211	400	202
0.169–0.199	103	622		422	
0.140–0.151				440	205
0.120–0.130		662		553	206
0.106					425

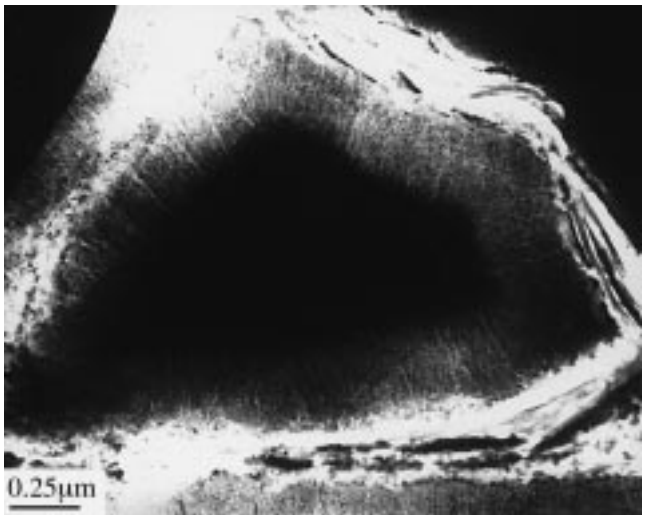

Fig. 6. Particle morphology of electrode after 400 cycles.

oxide layer into the matrix of the inner active material. It is obvious that these loose oxide layers cannot protect the particles from further attack by electrolyte and finally result in the continuous oxidation of the active materials.

4. Conclusions

The characteristics of $La_{0.65}Nd_{0.2}Pr_{0.15}Ni_{3.55}Co_{0.75}Mn_{0.4}Al_{0.3}$ electrode were investigated. The results show that $La_{0.65}Nd_{0.2}Pr_{0.15}Ni_{3.55}Co_{0.75}Mn_{0.4}Al_{0.3}$ alloy has suitable plateau pressure and fast activation capability. Surface composition analysis indicates that some elements such as La, Al, Mn and Co are in the form of La_2O_3, Al_2O_3, MnO and CoO, respectively, but Ni remains as pure metal. The results of high rate capability and cycle life tests suggest that substitution of La by an optimum amount of Nd and Pr may effectively improve discharge capacity and cycle life. In addition, the oxidation–pulverization–reoxidation phenomenon of the particles was observed by using AEM during charge–discharge cycling. It can be concluded that the mechanism of cycle life degradation is due to the combined effect of oxidation and pulverization.

Acknowledgement

The authors are grateful to Dr F.G. Shi, University of California, Irvine, for his critical reading of the manuscript and helpful suggestions.

References

1. J.H.F. Vanvulcht and H.C.A.M. Burning, *Philips Res.* Rep. **25** (1970) 133.
2. J.J.G. Willems, *Philips J. Res.* **39** (1984) 1, suppl.1.
3. T. Sakai, K. Oguro, H. Miyamura, N. Kuriyama, A. Kato, H. Ishikawa and C. Iwakura, *J. Less-Common Met.* **161** (1990) 193.
4. T. Sakai, H. Miyamura, N. Kuriyama, A. Kata, K. Ogugo, H. Ishikawa and C. Iwakura, *J. Less-Common Met.* **159** (1990) 127.
5. T. Saikai, T. Hazama, H. Miyamura, N. Kuriyama, A. Kato and H. Ishikawa, *J. Less-Common Met.* **172–174** (1991) 1175.
6. H.M. Jin, Z.H. Wen, H.Y. Ren and G.X. Li, *Rare Earth (Chinese)* **21** (1997) 73.
7. P.H.L. Notten, R.E.F. Einerhand and J.L.C. Daams, *J. Alloys Comp.* **210** (1994) 221.
8. P. Wu and K.L. Heng, *Chem. Mater.* **11** (1999) 858.